Supporting Information for:

Optimal separation method for high-precision K isotope analysis by using MC-ICP-MS with a dummy bucket

Xiaoqiang Li, [a] Guilin Han, *[a] Qian Zhang [a, b] and Zhuang Miao [c]

[a.] Institute of Earth Sciences, China University of Geosciences (Beijing), Beijing 100083, China.

[b.] Institute of Geographic Sciences and Natural Resources Research, Chinese Academy of Sciences, Beijing 100101, China.

[c.] School of Earth Science and Resources, China University of Geosciences, Beijing 100083, China.

*Corresponding author E-mail: hanguilin@cugb.edu.cn.

Xiaoqiang Li: xiaoqli@cugb.edu.cn.

Contents of this file

Introduction

This supporting information provides the detailed description of methodology, figures and tables to support the results presented in the main text.

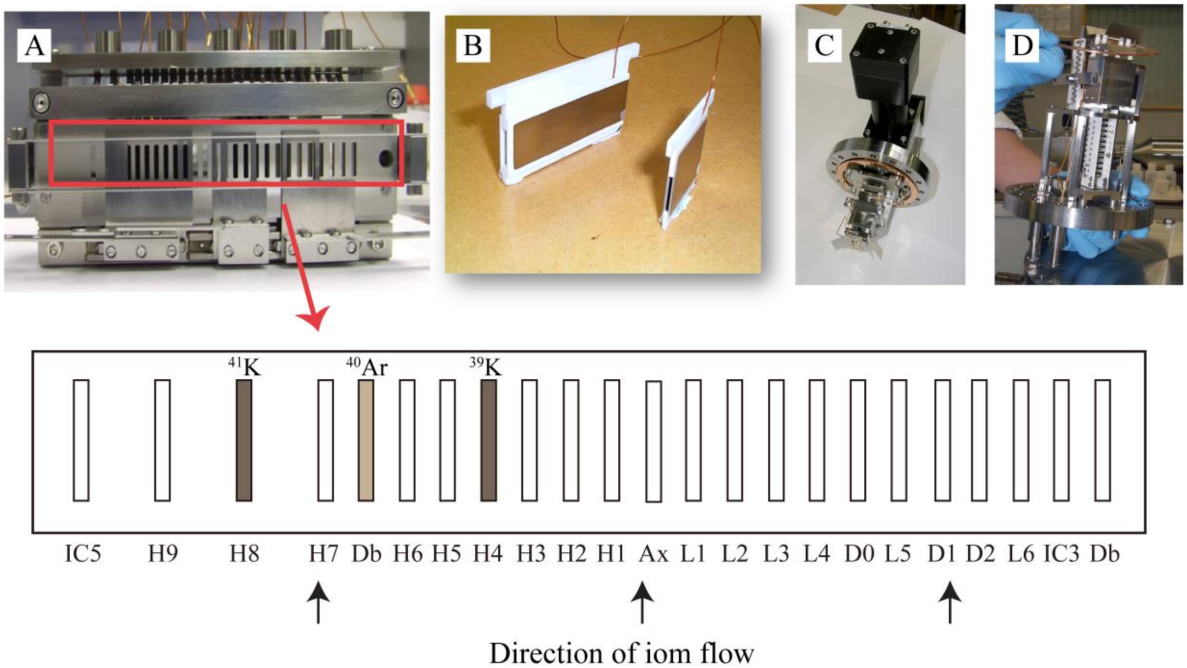

Figure S1. (A) Arrangement diagram of cups, dummy bucket and Daly detectors.; (B) Faraday detectors (H9-L6); (C) Daly detectors (D0-D2); (D) Ion counting detectors (IC3 and IC5).

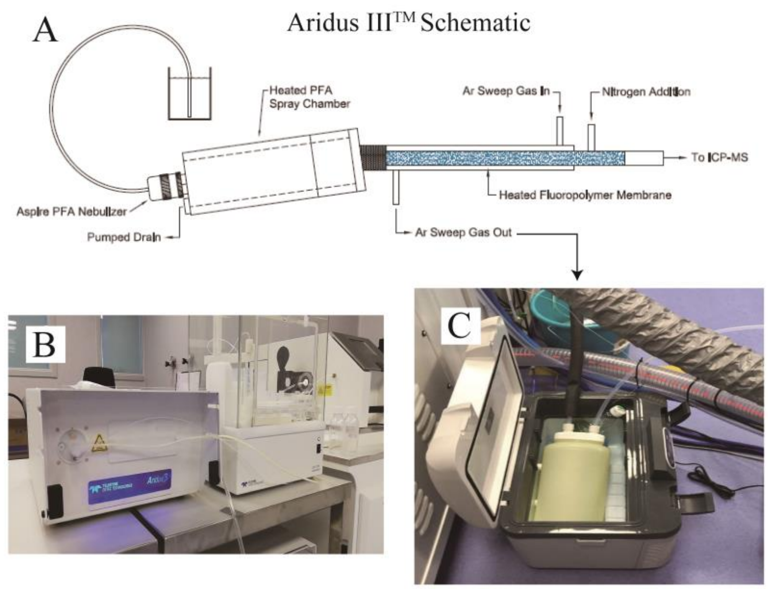

Figure S2. (A) A schematic drawing of CETAC Aridus III; (B) CETAC ASX-112FR autosampler and CETAC Aridus III; (C) KEMIN Electric refrigerator.

High Resolution

The Nu Plasma 3 has true high-resolution capabilities made possible by simultaneous application of three sets of adjustable slits, positioned at various points on the instruments, Figure 3. These slits consist of a source slit, which has 3 selectable width settings of 0.3, 0.05 and 0.03 mm; An alpha slit which is fully adjustable from 0-7mm using 'muscle wire' technology controlled from the Nu Plasma software (alpha 1 and alpha 2); and collector slits which are positioned in front of a few specifically chosen collectors, and operate from 0-1mm.

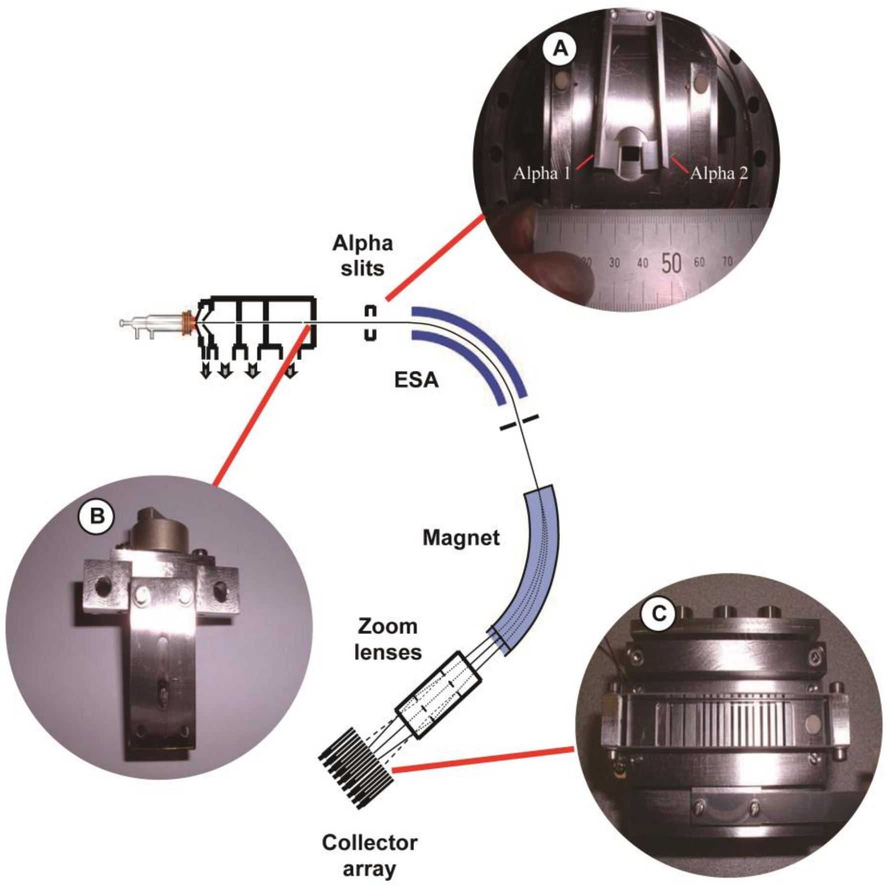

Figure S3. (A) Alpha (B) Source, and (C) Collector slit photographs and their respective location on a Nu Plasma instrument, the figure is from Nu Instruments Ltd.

Figure S4A illustrates the importance of narrowing the collector and source slits to achieve true high resolution. The necessity to narrow the alpha slit is less obvious to appreciate but is as equally important as the other two slits. Basically, the alpha slit reduces beam aberrations caused by a diverging beam entering the magnet producing a blurred image at the collector. Typically, the alpha slit is adjusted until the beam intensity is halved. If no beam aberrations existed then the beam width at the collector would be solely dictated by the source slit width.

Pseudo High Resolution

In the pseudo high resolution mode, the source slit and alpha slits are adjusted as for true high resolution to give two specially resolved beams at the collector, figure S4B. However, instead of narrowing the collector slit in order to allow only one beam at a time to enter the Faraday cup, the interfering beam is simply clipped on one side of the collector slit while the analyte beam is collected. It is clear from comparing figures S4A and S4C that pseudo high resolution gives more analyte peak top flat than true high resolution for the same transmission.

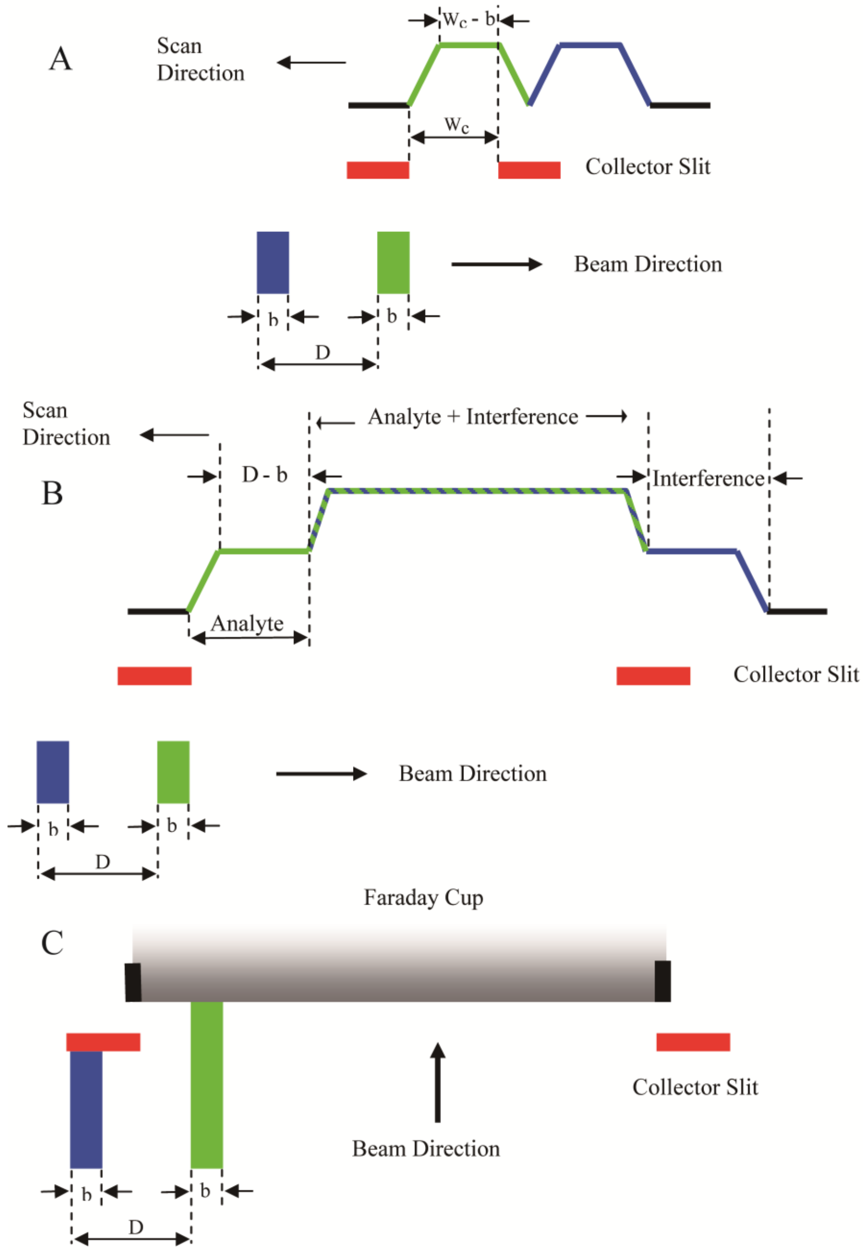

Figure S4. (A) Resultant peak shape after two specially resolved beams with dispersion D and width b are swept over a Faraday cup with collector slit width Wc.; (B) Resultant peak shape after two specially resolved beams with dispersion D and width b are swept over a Faraday cup with the collector slits fully open; (C) Magnet set so only the analyte beam is allowed to enter the Faraday cup while the interfering beam is clipped on the left hand collector slit. The figure is from Nu Instruments Ltd.

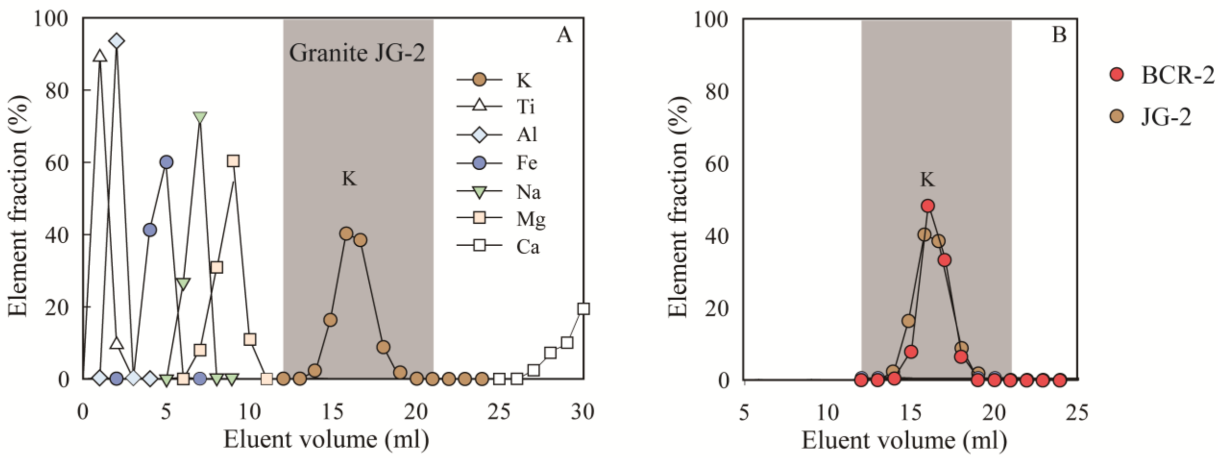

Figure S5. (A) Elution curves of K for granite JG-2 (A) and (B) are collection cuts processed for basalt BCR-2 and granite JG-2, respectively.

Table S1. Published single/multi-step potassium separation methods.

Reference	Step	Elution regent	Flow rate	Elution volume	Resin	Mesh	Diameter	Height	Volume of resin
1	one	0.5 M HNO_3	3.0 ml min^{-1}	700-1000 ml	AG50W-X8	200-400	25 mm	n.d. [a]	90 ml
2	one	0.5 M HNO_3	0.5 ml min^{-1}	80-250 ml	AG50W-X8	100-200	11 mm	n.d.	11 ml
3	one	1 M HNO_3	n.d.	n.d.	AG50W-X8	n.d.	n.d.	n.d.	1.8 ml
4	two	1.5 M HNO_3	n.d.	4.5-16.5 ml	AG50W-X12	100-200	4 mm	10 cm	1.3 ml
		0.5 M HNO_3	n.d.	6.5-15.5 ml	AG50W-X8	100-200	4 mm	4.2 cm	0.5 ml
5	one	0.5 M HNO_3	0.4-0.6 ml min^{-1}	180-340 ml	AG50W-X8	100-200	10 mm	n.d.	13 ml
	one	0.5 M HNO_3	0.5 ml min^{-1}	29-48 ml	AG50W-X8	100-200	4 mm	n.d.	1.6 ml
6	one or two	0.5 M HNO_3	n.d.	14-35 ml	AG50W-X8	200-400	8 mm	4 cm	2 ml
7	two	0.7 M HNO_3	n.d.	83-199 ml	AG50W-X8	100-200	15 mm	n.d.	17 ml
		0.5 M HNO_3	n.d.	15-37 ml	AG50W-X8	100-200	5 mm	n.d.	2.4 ml
This study	one	2 M HCl	0.05 ml min^{-1}	13-20 ml	AG50W-X12	200-400	4 mm	18 cm	2.3 ml

References

1. M. Humayun and R. N. Clayton, *Geochimica et Cosmochimica Acta*, 1995, **59**, 2131-2148.
2. M. Humayun and R. N. Clayton, *Geochimica et Cosmochimica Acta*, 1995, **59**, 2115-2130.
3. F. M. Richter, R. A. Mendybaev, J. N. Christensen, D. Ebel and A. Gaffney, *Meteoritics & Planetary Science*, 2011, **46**, 1152-1178.
4. W. Li, B. L. Beard, S. Li, *Journal of Analytical Atomic Spectrometry*, 2016, **31**, 1023-1029.
5. K. Wang, S. B. Jacobsen, *Geochimica et Cosmochimica Acta*, 2016, **178**, 223-232.
6. Y. Hu, X.-Y. Chen, Y.-K. Xu, F.-Z. Teng, *Chemical Geology*, 2018, **493**, 100-108.
7. H. Chen, Z. Tian, B. Tuller-Ross, Korotev, L. Randy; K. Wang, *Journal of Analytical Atomic Spectrometry*, 2019, **34**, 160-171.

Table S2. Test of influences of acid molarity, concentration mismatch on potassium isotopic analysis.

Name	$\delta^{41}K$	2SD	N	Name	$\delta^{41}K$	2SD	N
Acid mismatch test				Concentration mismatch test			
$A_{sample}/A_{standard}$				$C_{sample}/C_{standard}$			
0.50	0.51	0.09	4	0.50	0.32	0.06	4
0.80	0.14	0.06	4	0.70	0.21	0.05	4
0.90	0.09	0.05	4	0.80	0.16	0.07	4
0.95	0.04	0.05	4	0.90	0.15	0.06	4
1.00	0.03	0.06	4	0.95	0.02	0.04	4
1.05	−0.04	0.07	4	1.00	0.04	0.05	4
1.10	−0.06	0.05	4	1.05	0.03	0.06	4
1.20	−0.07	0.07	4	1.10	−0.06	0.06	4
1.50	−0.07	0.06	4	1.20	−0.11	0.05	4
				1.30	−0.13	0.07	4
				1.40	−0.12	0.06	4
				1.50	−0.15	0.09	4

Table S3. Test of influences of matrix elements on K isotopic analysis.

Name	%	$\delta^{41}K$	2SD	N	Name	%	$\delta^{41}K$	2SD	N
Na					Mg				
Na-1	0.1	−0.02	0.04	4	Mg-1	0.1	0.01	0.05	4
Na-2	1	−0.05	0.04	4	Mg-2	1	0.04	0.05	4
Na-3	2	−0.09	0.05	4	Mg-3	2	0.05	0.06	4
Na-4	5	−0.11	0.09	4	Mg-4	5	0.07	0.06	4
Na-5	10	−0.15	0.08	4	Mg-5	10	0.11	0.08	4
Ca					Cr				
Ca-1	0.1	−0.02	0.05	4	Cr-1	0.1	0.02	0.05	4
Ca-2	1	−0.01	0.06	4	Cr-2	1	−0.03	0.05	4
Ca-3	2	0.07	0.05	4	Cr-3	2	0.05	0.06	4
Ca-4	5	0.06	0.06	4	Cr-4	5	0.07	0.05	4
Ca-5	10	0.08	0.05	4	Cr-5	10	0.11	0.06	4
Ga					Rb				
Ga-1	0.1	0.03	0.04	4	Rb-1	0.1	0.03	0.04	4
Ga-2	1	0.04	0.04	4	Rb-2	1	0.04	0.04	4
Ga-3	2	−0.05	0.06	4	Rb-3	2	0.05	0.06	4
Ga-4	5	−0.07	0.05	4	Rb-4	5	0.07	0.05	4
Ga-5	10	−0.07	0.06	4	Rb-5	10	0.09	0.08	4

Table S4. K isotopic composition of geological and biological standards in this study and in the literature.

Sample	Reference	K (wt.%) [a]	$\delta^{41}K$	2SD	N
Seawater, Atlantic	This study	399 ppm	0.11	0.06	10
	Morgan et al.[1]		0.03	0.17	
	Li et al.[2]		0.05	0.17	
	Wang and Jacobsen[3]		0.10	0.31	
	Xu et al.[4]		0.14	0.03	
AGV-2, Andesite, USGS	This study	2.39	−0.38	0.04	3
			−0.44	0.02	3
			−0.41	0.04	3
Average			−0.41	0.06	9
	Li et al.[2]		−0.48	0.18	
AGV-1	Wang and Jacobsen[3]		−0.46	0.37	
AGV-1	Xu et al.[4]		−0.45	0.12	
AGV-1	Hu et al.[5]		−0.45	0.05	
AGV-1	Chen et al.[6]		−0.43	0.22	
BCR-2, Basalt, USGS	This study	1.49	−0.40	0.02	3
			−0.39	0.02	3
			−0.35	0.03	3
Average			−0.38	0.05	9
	Li et al.[2]		−0.51	0.19	
BCR-1	Xu et al.[4]		−0.40	0.04	
BCR-1	Hu et al.[5]		−0.42	0.06	
BCR-1	Chen et al.[6]		−0.49	0.12	
BHVO-2, Basalt, Hawaiian, USA	This study	0.43	−0.41	0.02	3
			−0.39	0.05	3
Average			−0.40	0.04	6
	Li et al.[2]		−0.50	0.19	
BHVO-1	Xu et al.[4]		−0.41	0.02	
BHVO-1	Hu et al.[5]		−0.43	0.06	
	Chen et al.[6]		−0.47	0.08	
GSP-2, Granodiorite, USGS	This study	4.48	−0.42	0.03	3
			−0.48	0.04	3
Average			−0.45	0.04	6
	Li et al.[2]		−0.50	0.12	
GSP-1	Wang and Jacobsen[3]		−0.41	0.24	
GSP-1	Xu et al.[4]		−0.48	0.12	
GSP-1	Hu et al.[5]		−0.50	0.04	
	Chen et al.[6]		−0.44	0.14	
JG-2, Granite, Japan	This study	2.24	−0.49	0.04	3
			−0.46	0.04	3
			−0.48	0.04	3
Average			−0.48	0.05	9
JG-1	Xu et al.[4]		−0.43	0.02	
RGM-2, Rhyolite, USGS	This study	3.61	−0.41	0.04	3
			−0.39	0.04	3
			−0.36	0.05	3
Average			−0.38	0.06	9

RGM-1	Xu et al.[4]		−0.38	0.03	
RGM-1	Chen et al.[6]		−0.35	0.15	
W-2a, diabase, USGS	This study	0.51	−0.43	0.05	3
			−0.39	0.05	4
Average			−0.41	0.06	7
	Xu et al.[4]		−0.39	0.03	
	Chen et al.[6]		−0.55	0.21	
SDC-1, Mica Schist, USGS	This study	2.69	−0.46	0.02	3
			−0.46	0.03	3
			−0.41	0.04	3
			−0.44	0.04	3
Average			−0.44	0.06	12
	Morgan et al.[1]		−0.49	0.09	
	Xu et al.[4]		−0.46	0.03	
DNC-1a, dolerite, USGS	This study	0.19	−0.32	0.02	3
			−0.35	0.02	3
Average			−0.33	0.03	6
JMS-2, Marine sediment, GSJ	This study	2.24	−0.33	0.05	3
			−0.30	0.02	3
			−0.32	0.05	6
GSB-6, Spinach leaves, IGGE	This study	2.49	−0.20	0.06	5
GSV-2, Bush leaves, IGGE	This study	0.92	0.04	0.03	4
GSB-14, Laver, IGGE	This study	3.36	0.25	0.07	4
GSS-2, soil, IGGE	This study	2.11	−0.54	0.04	4
GSS-3, soil, IGGE	This study	2.52	−0.38	0.04	4
GSS-4, soil, IGGE	This study	0.85	−0.46	0.07	3
GSS-6, soil, IGGE	This study	1.41	−0.85	0.08	4
GSS-8, loess, IGGE	This study	2.01	−0.39	0.03	3
GSD-6, stream, sediment, IGGE	This study	2.02	−0.45	0.05	3
GSD-11, stream, sediment, IGGE	This study	2.72	−0.48	0.07	3
GSD-12, stream, sediment, IGGE	This study	2.42	−0.55	0.07	3
GSD-14, stream, sediment, IGGE	This study	1.91	−0.31	0.06	3

References

1. L. E. Morgan, D. P. Santiago Ramos, B. Davidheiser-Kroll, J. Faithfull, N. S. Lloyd, R. M. Ellam, J. A. Higgins, *Journal of Analytical Atomic Spectrometry*, 2018, **33**, 175-186.
2. W. Li, B. L. Beard, S. Li, *Journal of Analytical Atomic Spectrometry*, 2016, **31**, 1023-1029.
3. K. Wang and S. B. Jacobsen, *Geochimica et Cosmochimica Acta*, 2016, **178**, 223-232.
4. Y. Xu, Y. Hu, X. Chen, T. Huang, R. S. Sletten, D. Zhu and F. Teng, *Chemical Geology*, 2019, **513**, 101-107.
5. Y. Hu, X.-Y. Chen, Y.-K. Xu, F.-Z. Teng, *Chemical Geology*, 2018, **493**, 100-108.
6. H. Chen, Z. Tian, B. Tuller-Ross, Korotev, L. Randy; K. Wang, *Journal of Analytical Atomic Spectrometry*, 2019, **34**, 160-171.